

Subcutaneous Infection with Non-mouse Adapted Dengue Virus D2Y98P Strain Induces Systemic Vascular Leakage in AG129 Mice

Grace KX Tan,¹*MSc*, Jowin KW Ng,¹*BSc*, Angeline HY Lim,¹*BSc*, Kim Pin Yeo,¹*BSc*, Veronique Angeli,¹*PhD*, Sylvie Alonso¹*PhD*

Abstract

Introduction: Dengue (DEN) is a mosquito-borne viral disease which has become an increasing economic and health burden for the tropical and subtropical world. Plasma leakage is the most life threatening condition of DEN and may lead to hypovolaemic shock if not properly managed. **Materials and Methods:** We recently reported a unique dengue virus strain (D2Y98P) which upon intraperitoneal (IP) administration to immunocompromised mice led to systemic viral dissemination, intestine damage, liver dysfunction, and increased vascular permeability, hallmarks of severe DEN in patients (Tan et al, PLoS Negl Trop Dis 2010;4:e672). **Results:** Here we report the clinical manifestations and features observed in mice subcutaneously (SC) infected with D2Y98P, which is a route of administration closer to natural infection. Similar to the IP route, increased vascular permeability, intestine damage, liver dysfunction, transient lymphopenia (but no thrombocytopenia) were observed in the SC infected mice. Furthermore, the SC route of infection was found more potent than the IP route whereby higher viral titers and earlier time-of-death rates were measured. In addition, various staining approaches revealed structurally intact blood vessels in the moribund animals despite pronounced systemic vascular leakage, as reported in dengue hemorrhagic fever/dengue shock syndrome (DHF/DSS) patients. Interestingly, measurement of soluble mediators involved in vascular permeability indicated that vascular leakage may occur at an early stage of the disease, as proposed in DEN patients. **Conclusion:** We believe that this novel mouse model of DEN-associated vascular leakage will contribute to a better understanding of DEN pathogenesis and represents a relevant platform for testing novel therapeutic treatments and interventions.

Ann Acad Med Singapore 2011;40:523-32

Key words: Dengue shock syndrome, Dengue hemorrhagic fever, Capillary leakage

Introduction

Dengue (DEN) is an arthropod-borne viral disease that is endemic in subtropical and tropical countries.¹ The highly domesticated *Aedes aegypti* mosquito is the main vector for DEN virus (DENV) transmission to humans. With approximately half the world's population residing in DEN endemic regions² and more than 50 million new infections estimated to occur annually,³ DEN certainly poses a global health threat.

DENV infections may be asymptomatic or lead to undifferentiated fever, dengue fever (DF) or dengue

hemorrhagic fever (DHF) with plasma leakage that may lead to hypovolaemic shock (dengue shock syndrome, DSS). According to the 1997 World Health Organization guidelines (<http://www.who.int/topics/dengue/en/>), all 4 clinical/laboratory criteria, fever, hemorrhagic tendency, thrombocytopenia, and capillary leakage must be fulfilled for DHF/DSS classification. In DHF/DSS patients, capillary leakage is often observed at the time of defervescence and develops rapidly over a period of hours. Pleural effusion, ascites and hemoconcentration (hematocrit increased by more than 20%) are indicative of leakage.⁴ The patient can

¹Department of Microbiology, Immunology Programme, National University of Singapore

Address for Correspondence: Assistant Professor Sylvie Alonso, Immunology Programme, Department of Microbiology, 28 Medical Drive, CeLS #03-05, Singapore 117597.

Email: micas@nus.edu.sg

quickly progress to shock if volume loss is not remedied with proper fluid therapy and severe leak will be accompanied by cardiovascular collapse within hours.

Bleeding tendencies are also observed in DSS patients: hemorrhagic manifestations range from a positive tourniquet test to the presence of petechiae, ecchymosis or purpura and/or spontaneous bleeding mainly from the mucosa and gastrointestinal tract. Hemoconcentration and marked thrombocytopenia (platelet count $<100 \times 10^9/L$) are the 2 hallmarks of DHF/DSS.⁵ Hepatic involvement has also been implicated in DEN disease which translates into elevated levels of aspartate (AST) and alanine (ALT) transaminases.⁶ While the haematological, vascular and hepatic systems appear to be central in the DHF/DSS pathology,⁷ atypical clinical presentations that involve other organs have been increasingly reported, including encephalitis, myocarditis and cholecystitis.⁸⁻¹⁰

The current paradigm that explains increased vascular permeability in DEN patients involves a variety of soluble mediators known to play a role in vascular permeability based on measurements in DEN patients and, in some cases, further supported by *in vitro* experiments using endothelial cell lines.^{11,12} They include pro-inflammatory cytokines and chemokines, metalloproteinases (MMP),¹³ complement proteins,¹⁴ vascular endothelial growth factor A (VEGF-A) and its receptor VEGFR-2,¹⁵ nitric oxide, tissue fibrinogen activator, endothelin, thrombomodulin, dengue virus non-structural protein 1 (NS1), and cross-reactive anti-NS1 antibodies. In addition, an *in vitro* proteomic approach recently showed that DENV induces F-actin re-organisation in endothelial cells and modulates the expression and redistribution of surface molecules that play a critical role in vascular permeability.¹⁶ The current paradigm for DEN associated vascular leakage thus involves the combination of a plethora of soluble factors that act in concert and lead to the transient alteration of the vascular permeability. However, note that most of the dysfunctions such as elevated levels of pro-inflammatory cytokines and chemokines for example, proposed to play a critical role in vascular leakage during DEN disease, have been reported in other infections but without a noticeable effect on the vascular permeability. Moreover, general lack of structural changes and alterations of the blood vessels in DEN patients argues against some of the proposed mechanisms such as the destructive role of MMPs on the blood vessels or the apoptotic function of tumor necrosis factor- α (TNF- α) on endothelial cells. Therefore, some pieces are clearly missing in the current paradigm to fully explain what causes vascular leakage in DEN patients.

Progress in deciphering the mechanisms responsible for DEN pathogenesis and in developing effective prophylactic and/or therapeutic treatments has been impeded by the lack of

a relevant and convenient animal model.¹⁷ Most of the DENV strains do not replicate efficiently in immunocompetent mice. Mouse-adapted DENV strains displayed a higher infectivity but led to irrelevant clinical manifestations such as paralysis.^{18,19} Alternatively, immunocompromised mice displayed greater susceptibility to DENV infection.²⁰⁻²³ Among them, AG129 mice, deficient in interferon (IFN)- α/β and - γ receptors, allowed effective replication of DENV.^{24,25} We have recently described a unique non-mouse adapted DENV serotype 2 strain, namely D2Y98P, which is highly infectious in AG129 mice.²⁶ Infection via the intraperitoneal (IP) route with a relatively low dose (10^4 plaque forming unit, PFU) of this virus led to asymptomatic viral dissemination and replication in relevant organs, followed by non-paralytic death of the animals after the virus had cleared from the blood circulation, similar to the disease kinetic observed in humans. Intestine damage, liver dysfunction and increased vascular permeability were observed in the infected animals. We report here the clinical manifestations and features of AG129 mice infected with the same virus via the subcutaneous (SC) route, closer to natural infection.

Materials and Methods

Virus strain and growth conditions. The D2Y98P-PP1 virus used in this study was derived from the D2Y98P strain that had been plaque-purified twice sequentially on BHK-21 cells and fully sequenced (Genbank accession number #JF327392).²⁷ D2Y98P-PP1 virus was propagated in C6/36 cells (ATCC# CRL-1660) as described previously.²⁵ Virus stocks were stored at -80°C .

Plaque assay

Plaque assay was carried out in BHK-21 cells as described previously.²⁶ Briefly, 2×10^5 cells BHK-21 cells were seeded in 24-well plates (NUNC, NY, USA). BHK-21 monolayers were infected with 10-fold serially diluted viral suspensions ranging from 10^{-1} to 10^{-8} . After 1 hour incubation at 37°C and 5% CO_2 , the medium was decanted and 1% (w/v) carboxymethyl cellulose was added to the wells. After 4 days incubation at 37°C and 5% CO_2 , the cells were fixed with 4% paraformaldehyde and stained with 1% crystal violet. The plates were dried and the plaques were scored visually and expressed as the number of plaque forming units (PFU). Triplicate wells were run for each dilution of each sample. The limit of detection for the plaque assay was set at 10 PFU per ml or per g of tissue.

Mice infection

All the animal experiments were carried out under the guidelines and upon approval of the animal ethics

committees from the National University of Singapore (NUS). Blood withdrawal procedure was performed under anesthesia, and all efforts were made to minimise suffering. AG129 [129/Sv mice deficient in both alpha/beta (IFN- α / β) and gamma (IFN- γ) interferon receptors] were obtained from B&K Universal (UK). They were kept under specific pathogen-free conditions in individual ventilated cages. Eight to nine week-old mice were administered with 10^7 to 10^4 PFU of D2Y98P-PP1 via the SC route (0.1 ml in PBS) in the back's skin. Survival rate was derived from the number of mice that were euthanised at moribund stage as evidenced by severe diarrhea and lethargy as described previously.²⁶

Determination of virus titres in infected mice

Blood samples were collected from the cheek vein in 0.4% sodium citrate and centrifuged for 5 minutes at 6000 g to obtain plasma. The presence of infectious viral particles was determined by plaque assay as described above. The levels of infectious virus in the tissues from infected mice were assessed as described previously.²⁶ Briefly, euthanised animals were perfused systemically with PBS prior to harvesting the liver, spleen, brain, spinal cord, kidney, back's skin, intestines, mesenteric lymph nodes, brachial and axillary lymph nodes. Ten-fold serial dilutions of each tissue homogenate (from neat to 1: 10^5) were assayed in a standard virus plaque assay on BHK-21 cells as described above. Triplicate wells were run for each dilution of each sample. Data are expressed as log₁₀ [mean \pm SD] in PFU per gram of wet tissue with a limit of sensitivity set at 1.0 log₁₀ PFU/g of tissue. Five mice per time point per group were assessed. Results are representative of at least 2 independent experiments.

Histology

Mice were euthanised, and tissues were harvested and immediately fixed in 10% formalin in PBS. Fixed tissues were paraffin embedded, sectioned and stained with hematoxylin and eosin (H&E).

Vascular permeability assay

Vascular leakage was assessed using Evans Blue dye as a marker for albumin extravasation as described previously.²⁶ Briefly, 0.2 ml of Evans blue dye (0.5 % w/v in PBS) (Sigma Aldrich) were injected intravenously into the anaesthetised mice. After 2 hours, the animals were euthanised and extensively perfused with PBS. The tissues were harvested and weighed prior to dye extraction using N,N-dimethylformamide (Sigma; 4ml/g of tissue wet weight) at 37°C for 24 hours after which absorbance was read at 620nm. Data are expressed as fold increase in

OD620nm per gram of tissue wet weight compared to the uninfected control.

Hematology

Mouse blood samples were collected in K2EDTA and serum tubes (Biomed Diagnostics). Serum alanine (ALT) and aspartate (AST) aminotransferases, and albumin levels were quantified using chemistry analyser COBAS C111 (ROCHE).

Detection of cytokines and other soluble mediators

TNF- α , Interleukin-6 (IL-6), MMP2, MMP9, VEGF-A, VEGFR-2 and C5a were measured in the serum of infected and uninfected mice using specific detection kits (R&D).

Visualisation of vascular endothelium using DiI dye

Blood vessels can be directly labelled with 1,1'-dioctadecyl-3,3,3',3'-tetramethylindocarbocyanine perchlorate (DiI), a lipophilic carbocyanine dye, which is incorporated into the endothelial cell membranes upon contact.²⁸ Briefly, cardiac perfusion of various solutions in the following order was administered to the euthanised mice at a rate of 1 to 2 ml/min: 2 ml of PBS, then 5 ml of DiI solution and finally, 10 ml of 4% paraformaldehyde fixative. Whole animal tissues were then observed under a fluorescence microscope (Olympus) using a rhodamine filter set.

Visualisation of vascular endothelium by immunohistochemistry

Whole-mount immunohistochemical analysis of the intestines was performed as described previously.²⁹ Mice were euthanised and perfused with 4% paraformaldehyde. Tissues were dissected and further fixed in 4% paraformaldehyde overnight at 4°C. Fixed tissues were then incubated overnight at 4°C in a blocking solution of 0.5% bovine serum albumin and 0.3% Triton X-100 in PBS. Finally, tissues were incubated with anti-rat CD31 antibody (PECAM-1; BD Biosciences San Jose, CA) and revealed by Cy3-conjugated anti-rat antibody (Jackson ImmunoResearch). Specimens were viewed under a fluorescence microscope (Axio imager.Z1, AxioCam HRM camera; Carl Zeiss Micro Imaging, Inc., Jena, Germany).

Statistics

All statistical analysis was done with GraphPad Prism Version 5.0 (GraphPad Software, San Diego, CA, USA). Data were analysed by Student's t test. A one-tailed $P < 0.05$ was considered significant.

Results

Survival rate and viremia in D2Y98P-PP1-infected AG129 mice

To test the infectious potential of the D2Y98P-PP1 strain when administered via the SC route, AG129 mice were infected with 10-fold serially diluted viral doses ranging from 10^2 to 10^7 PFU. Survival rates indicated that SC infection with as few as 10^3 PFU and above led to 100% mortality (Fig. 1). As previously reported for the IP route,²⁶ a direct correlation between viral dose and time-of-death was observed, which ranged between 6 to 16 days p.i. for the 10^7 to 10^3 PFU viral dose range. SC infection with 10^2 PFU gave 10% survival only (Fig. 1A). The clinical manifestations that were observed upon SC infection were similar to those observed upon IP infection²⁶ i.e. ruffled fur and hunched posture which further progressed to lethargy, diarrhea-like symptoms and moribundity at which stage the animals were euthanised. No signs of paralysis were observed. In order to compare with the IP route of infection previously reported,²⁶ we monitored the viremia over time in the animals SC infected with 10^4 PFU of D2Y98P-PP1 virus. A peak of viremia was observed at day 5-6 p.i. followed by viral clearance at the time of the animals' death by day 12 p.i. (Fig. 1B).

Tissue tropism and kinetic of virus replication in D2Y98P-PP1-infected AG129 mice

Upon SC infection with 10^4 PFU of D2Y98P-PP1 virus, the presence of infectious viral particles was monitored over time and quantified in the back's skin, brachial and axillary

lymph nodes, liver, intestines, mesenteric lymph nodes, spleen, brain, spinal cord and kidneys. The animals were perfused prior to organ and tissue harvest, thereby ensuring that the number of PFU obtained represents the number of virus particles that have reached the organs and tissues. The infection profiles observed in the skin, liver, intestines, spleen and kidneys followed the viremia (compare Figs. 2A, C, D, F, I with Fig 1B). In contrast, high levels of infectious viral particles were still detected at moribund state in the brachial and axillary lymph nodes (Fig. 2B), mesenteric lymph nodes (Fig. 2E), brain (Fig. 2G) and spinal cord (Fig. 2H). Even more interestingly, whereas for most of the organs tested a peak of virus concentration was detected at day 5-6 p.i. followed by more or less rapid clearance, the concentration of infectious viral particles kept increasing over time in the brain and spinal cord (Figs. 2G and H).

Histology of intestines, spleen, liver and brain from D2Y98P-PP1-infected AG129 mice

Histological analysis revealed severe damage of the intestines as early as day 6 p.i. with detachment and disintegration of the intestinal villi (Fig. 3A). In contrast, the liver and spleen architecture did not appear significantly altered throughout the infection. However, hepatic necrosis was observed at day 11 p.i., characterised by pyknotic nuclei and cytoplasmic vacuolation of hepatocytes. Liver damage was further supported by elevated levels of alanine (ALT) and aspartate (AST) transaminases in the infected animals (Fig. 3B). Signs of vacuolation were also observed in the cerebellum at day 11 p.i., indicative of some brain tissue damage (Fig. 3A).

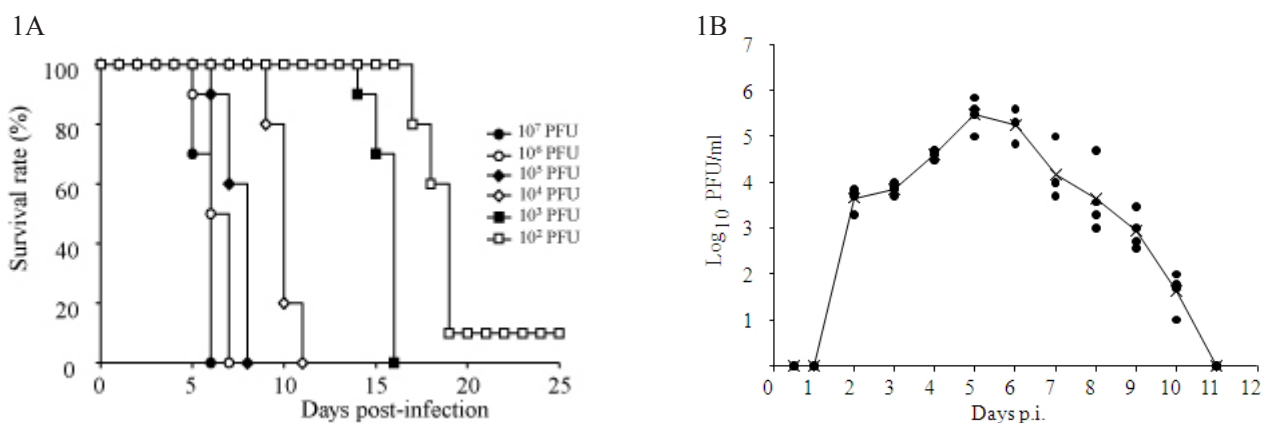


Fig. 1. Survival rate and viremia in D2Y98P-PP1-infected mice. Fig. 1A shows the survival rate of 8-9 weeks old AG129 mice that were infected subcutaneously (SC) with 10-fold serially diluted suspensions of D2Y98P-PP1 virus as indicated. Survival rate was monitored over time post-infection (p.i.). Ten mice per group were used. Fig. 1B shows viremia in AG129 mice that were SC infected with 10^4 PFU of D2Y98P-PP1 strain. Viremia was monitored over time post-infection. Five animals were sacrificed at each time point. Blood was collected and the number of infectious viral particles was determined by plaque assay in BHK cells. The limit of detection is set at 10 PFU per ml. Legend: black circles represent individual virus titers measured at each time point for each mouse; and crosses represent the average of the virus titers at each time point.

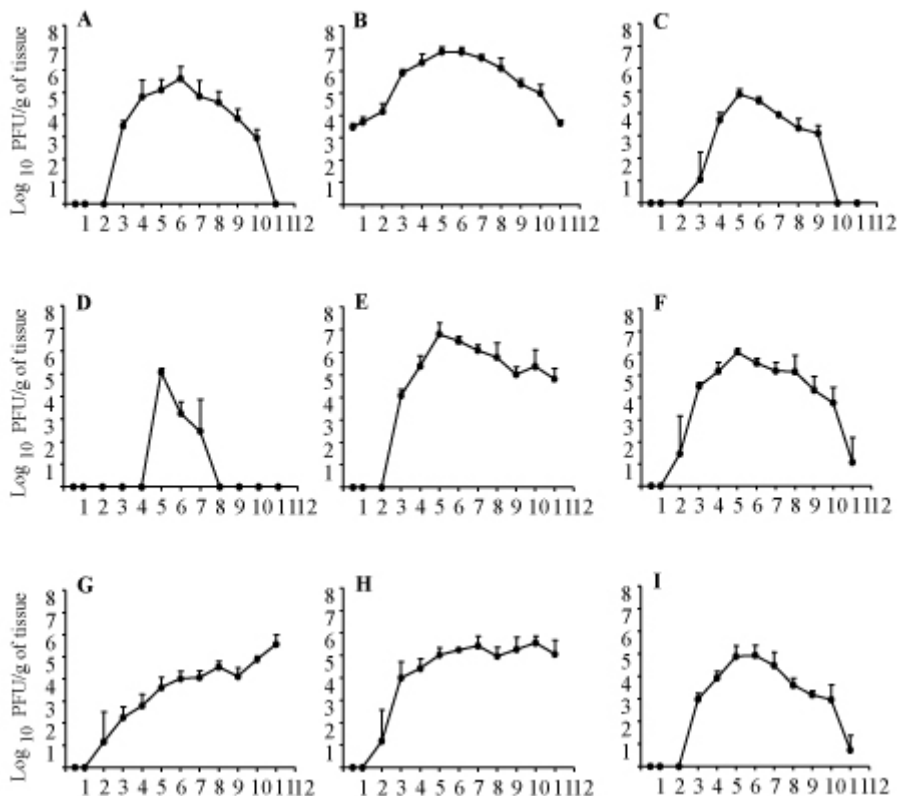


Fig. 2. Kinetic of infectious virus particles in organs and tissues from D2Y98P-PP1-infected mice. AG129 mice were subcutaneously (SC) infected with 10^4 PFU of D2Y98P-PP1 strain. At the indicated time points p.i., 5 animals were sacrificed, perfused with PBS and (A) the back's skin, (B) brachial and axillary lymph nodes, (C) liver, (D) intestines, (E) mesenteric lymph nodes, (F) spleen, (G) brain, (H) spinal cord and (I) kidneys were harvested and homogenised. The number of infectious viral particles was quantified by plaque assay. The limit of detection is set at 10 PFU per gram of tissue.

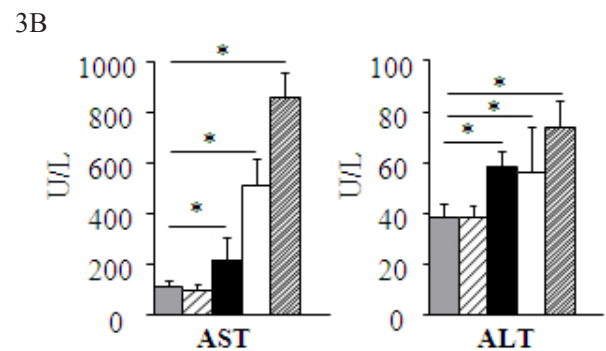
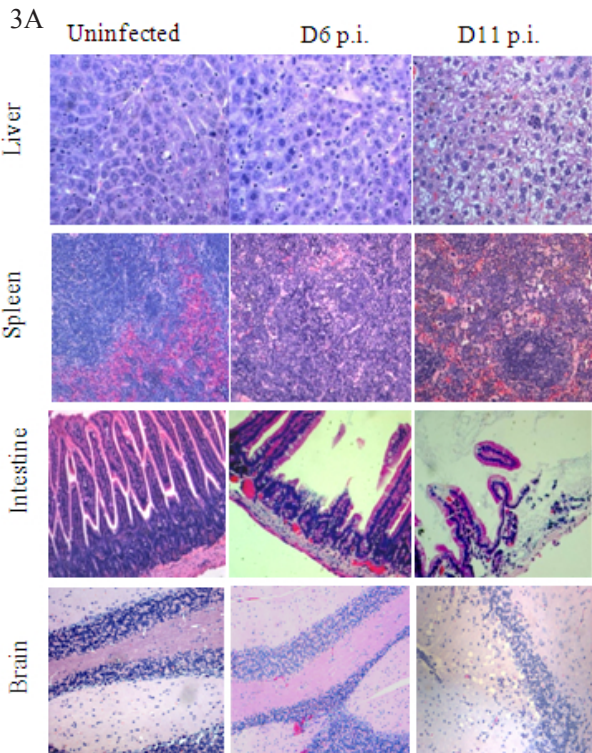


Fig. 3. Histology of intestines, liver, spleen and brain from D2Y98P-PP1-infected mice. Fig. 3A: AG129 mice were subcutaneously (SC) infected with 10^4 PFU of D2Y98P-PP1 strain or left uninfected. At day 6 and 11 p.i., the animals were sacrificed and their organs were harvested, fixed and processed for H&E staining. Observations were made at 200x (intestines and spleen), 400x (liver), and 100x (brain) magnification. Fig. 3B: Serum concentration of aspartate (AST) and alanine (ALT) transaminases. Legend: day 3 p.i. (broad striped bar); day 6 p.i. (black bar); day 9 p.i. (white bar); day 11 p.i. (narrow striped bar); and uninfected animals (grey bar).

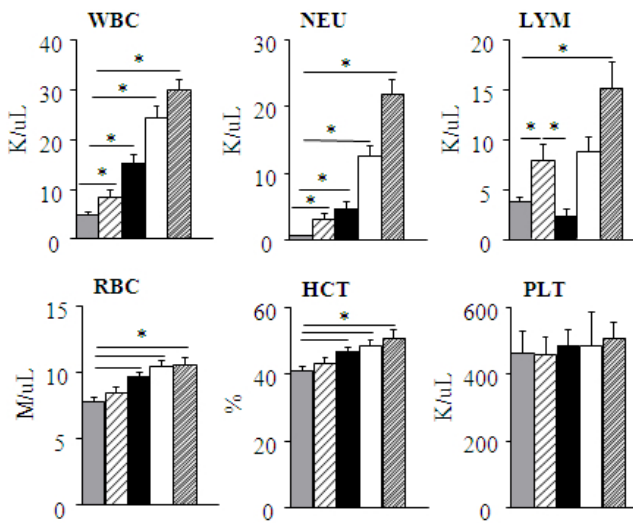


Fig. 4. Blood parameters in D2Y98P-PP1-infected mice. AG129 mice were subcutaneously (SC) infected with 10^4 PFU of D2Y98P-PP1 strain. At the indicated time points p.i., 5 mice were sacrificed and the blood was harvested for the measurement of blood parameters including white blood cells (WBC), neutrophils (NEU), lymphocytes (LYM), red blood cells (RBC), hematocrit (HCT), and platelet (PLT). Legend: day 3 p.i. (broad striped bar); day 6 p.i. (black bar); day 9 p.i. (white bar); day 11 p.i. (narrow striped bar); and uninfected animals (grey bar).

Blood parameters in D2Y98P-PP1-infected AG129 mice.

Various blood parameters were assessed over time post-infection in the SC infected animals and compared to the uninfected animal controls. They included white blood cells (WBC), neutrophils (NEU), lymphocytes (LYM), red blood cells (RBC), hematocrit (HCT), and platelets (PLT). WBC, NEU, RBC and HCT displayed increased concentrations throughout the course of infection which indicated cellular activation/proliferation and infiltration (WBC and NEU), and hemoconcentration (RBC and HCT) (Fig. 4). In contrast, the PLT concentration remained unchanged. A transient drop in LYM concentration was observed at day 6 p.i. followed by a sharp increase to reach at moribund state higher levels than those measured in the uninfected controls (Fig. 4).

Vascular leakage in D2Y98P-PP1-infected AG129 mice

Vascular leakage was first assessed in the SC infected animals using Evan’s blue dye extrusion assay as reported previously.²⁶ The results revealed a significant increase in the vascular permeability for all the organs tested (liver, intestine, kidney, spleen, skin) compared to the uninfected control animals (Fig. 5A). Vascular leakage was apparent at day 6 p.i. and was more pronounced at moribund state (day 11 p.i.). Consistently, significant decrease in the serum albumin concentration was observed in the infected animals, indicative of plasma proteins leakage (Fig. 5B).

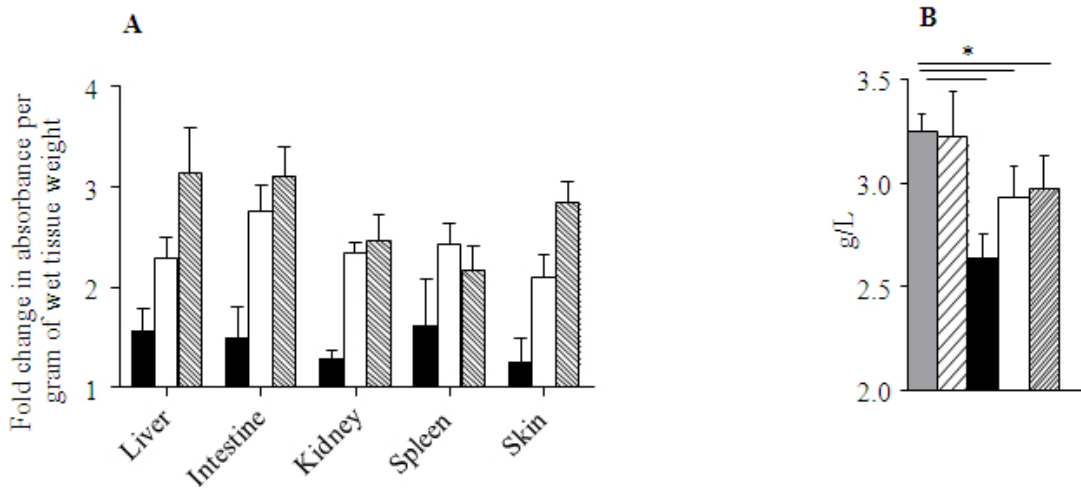


Fig. 5. Vascular leakage and serum albumin levels in D2Y98P-PP1-infected mice. Fig. 5A. At each indicated time point post-infection, 5 mice subcutaneously (SC) infected with 10^4 PFU of D2Y98P-PP1 strain were intravenously injected with Evan’s blue dye and sacrificed 2 hours later. After careful and extensive systemic perfusion with PBS, various organs and tissues were harvested and processed for Evan’s blue dye quantification. Results are expressed as fold changes compared to the uninfected animals control. Legend: day 6 p.i. (black bar); day 9 p.i. (white bar); and day 11 p.i. (striped bar). Fig. 5B. D2Y98P-PP1-infected and uninfected mice were bled at different time points p.i. to measure serum albumin concentration. Legend: uninfected (grey bar); day 3 p.i. (broad striped bar); day 6 p.i. (black bar); day 9 p.i. (white bar); and day 11 p.i. (narrow striped bar).

The current paradigm of DEN-associated vascular leakage involves a number of soluble players including inflammatory cytokines and chemokines, as well as non-inflammatory mediators such as MMPs and complement proteins. A number of these soluble mediators were measured in the AG129 mice SC infected with D2Y98P-PP1 virus, including TNF- α , IL-6, VEGF-A, VEGFR-2, MMP9 and MMP2, and complement protein C5a. The results showed that all the mediators measured were present in higher concentrations in the serum from the infected mice compared to the uninfected controls (Fig. 6). These increased levels were detected as early as day 3 p.i. and were either transient with a peak at day 3 p.i. (TNF- α , VEGF-A, VEGFR-2), or sustained throughout the course of infection (IL-6, MMP9, MMP2, C5a). Interestingly, the levels of VEGFR-2 measured in the serum from the infected animals at day 9 and 11 p.i. were significantly lower than the level measured in uninfected controls, suggesting internalisation or down-regulation of the receptor.

Altogether, these data support that SC infection with D2Y98P-PP1 virus induces systemic vascular leakage in AG129 mice with early detection (day 3 p.i.) of elevated levels of a number of soluble mediators involved in vascular permeability.

Vascular endothelium integrity

Intact endothelium has been reported in DEN patients who experience increased vascular permeability.³⁰ To assess blood vessels and capillaries integrity in our mouse model, SC infected mice were anaesthetised at a late stage of infection (day 9 p.i.) and cardiac perfusion was performed with a lipophilic carbocyanine dye (DiI) shown to uniformly and stably stain blood vessels.²⁸ Whole mount preparation of the small intestines was prepared and directly examined under a fluorescence microscope using a Rhodamine filter set. Despite the severe damage of the intestinal luminal structure (in particular the villi) as evidenced in the H&E stained sections (Fig. 3A), the large blood vessels and capillaries displayed no obvious structural alteration (Figs. 7A and B). To confirm this observation, CD31-immunolabelling was also performed. CD31 (aka PECAM-1, Platelet Endothelial Cell Adhesion Molecule-1) is a 130 kDa integral membrane protein that is expressed constitutively on the endothelial surface as well as at inter-endothelial cell contacts. The vascular structure of the blood vessels in the small intestine from DEN infected animals was found to be morphologically undamaged with intact inter-endothelial junctions (Figs. 7C and D).

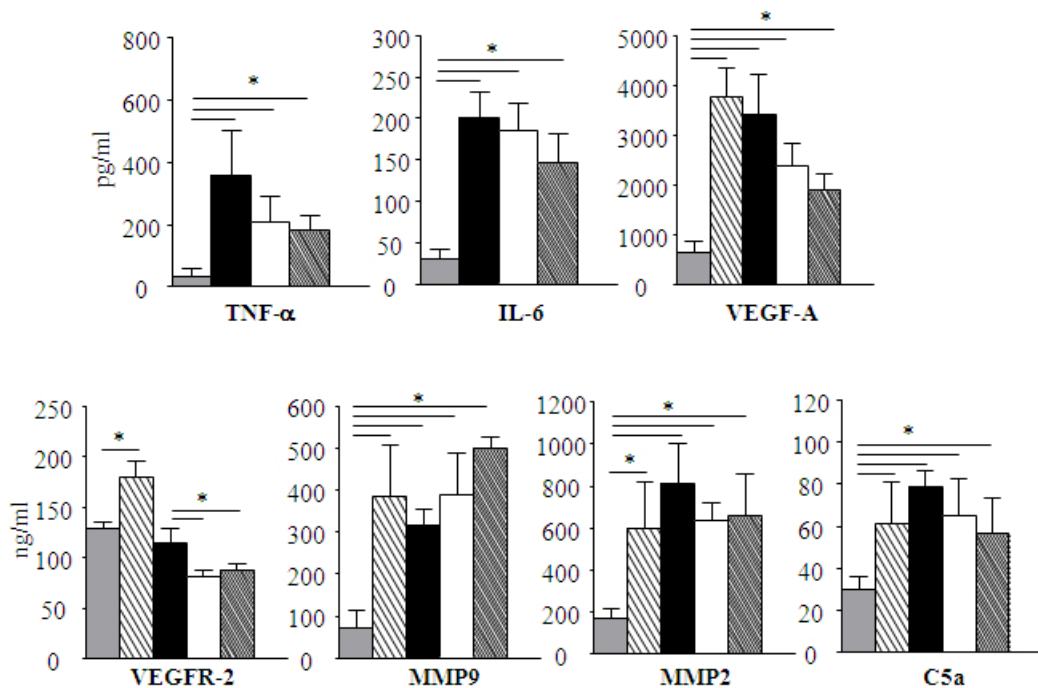


Fig. 6: Systemic levels of soluble mediators in D2Y98P-PP1-infected mice. AG129 mice were subcutaneously (SC) infected with 10^4 PFU of D2Y98P-PP1 strain. At the indicated time points p.i., 5 mice were sacrificed and the blood was harvested for measurements of various soluble mediators including TNF- α , IL-6, VEGF-A, VEGFR-2, MMP9, MMP2, and C5a as indicated. Legend: uninfected (grey bar); day 3 p.i. (broad striped bar); day 6 p.i. (black bar); day 9 p.i. (white bar); and day 11 p.i. (narrow striped bar).

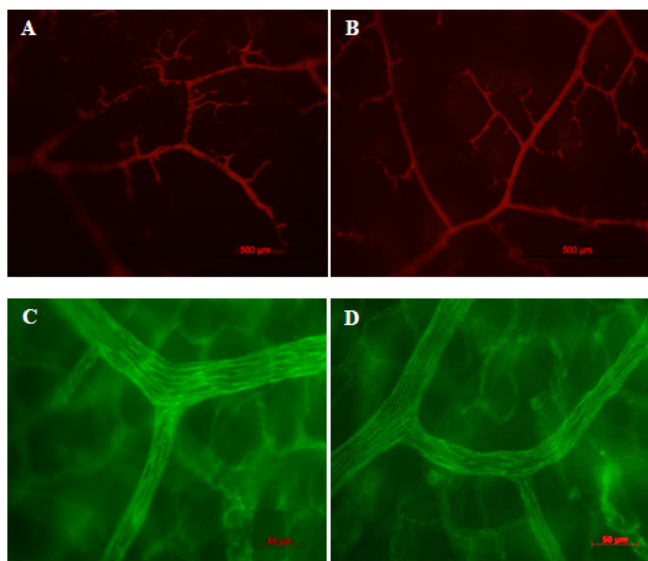


Fig. 7. Visualisation of the vascular endothelium in D2Y98P-PP1-infected mice. AG129 mice were SC infected with 10^4 PFU of D2Y98P-PP1 virus (panels B and D) or left uninfected (A&C). At moribund stage (Day 10 p.i.), the mice were anaesthetised and Dil dye was injected via cardiac perfusion before euthanasia (A & B). Whole mounts preparations of small intestines were made and directly observed under fluorescent microscope (A & B) or after staining with anti-CD31 antibody (C & D).

Discussion

We have previously reported the infection of AG129 adult mice with D2Y98P virus via the IP route.²⁶ We described here the clinical features and manifestations observed upon infection with the same virus via the SC route, closer to natural infection. Similar to the observations made with the IP route, SC infection led to a viral dose-dependent time-of-death of the animals which displayed comparable relevant clinical manifestations and features including transient viremia, intestine damage, liver dysfunction, transient lymphopenia, and increased vascular permeability. However, some important differences were observed between the SC and IP routes. Firstly, different time-of-death rates were observed in SC and IP infected mice infected with the same lethal viral dose. For example, IP infection with 10^4 PFU led to 100% mortality within 20 days p.i. versus 12 days in SC infected mice. As for sub-lethal viral doses, 90% versus 10% mortality rates were obtained in mice infected with 10^2 PFU via the SC and IP routes respectively. These observations thus suggested that the SC route of infection is more potent than the IP route at inducing severe disease in the mice. Secondly, for the same infectious dose (10^4 PFU), the peak concentrations of infectious viral particles measured systemically and in various organs from SC infected animals were at least 1 log higher than those measured in the IP infected mice.²⁶ This observation thus suggested a correlation between viral titers and disease severity in this mouse model of DEN, a

concept that is further supported by a recent work where we identified a single amino acid substitution in the viral genome responsible for the virulent phenotype of D2Y98P strain and which resulted in differential viral titers.²⁷ Furthermore, whereas no pathological signs were observed in the brain from IP infected animals, vacuolation was apparent in the cerebellum of the SC infected mice. Consistently, although relatively rare, DEN-associated encephalopathy has been reported before in humans.^{31,32} Brain tissue alteration in SC infected mice correlated with strikingly higher levels of infectious viral particles detected in their brain compared to the IP infected animals (6 log₁₀ PFU in SC infected animals versus 2 log₁₀ PFU in IP infected animals) and may be the result of a direct cytopathological effect of the virus.

The current paradigm that explains DEN-associated vascular leakage involves the combination of a plethora of soluble factors (including pro-inflammatory cytokines/chemokines and other non-inflammatory mediators) that act in concert and lead to the transient alteration of the vascular permeability.^{11,12} Consistently, transient or sustained elevated levels of TNF- α , IL-6, MMP2, MMP9, C5a, VEGF-A and VEGFR-2 were measured in the serum of the infected mice. Interestingly, these elevated levels were detected as early as day 3 p.i., which suggested that increased vascular permeability begins at a rather early stage of the disease. This hypothesis is supported by some early experimental evidence in DEN patients that alteration of the vascular permeability begins during the febrile phase of the illness.³⁰ However, due to the limited range of tools available to interrogate this phenomenon, plasma leakage is generally detectable and detected in DEN patients during or shortly after defervescence. Plasma leakage manifests via hemoconcentration tracked by increases of serial hematocrit measurements. Ultrasound examination has also proved useful to monitor plasma leakage.^{33,34} Furthermore, intact endothelium has been reported in DEN patients who experience increased vascular permeability.³⁰ Likewise, using Dil dye staining and anti-CD31 antibody labeling procedures, we showed that the blood vessels and capillaries from D2Y98P-infected mice appear intact even at moribund stage where vascular leakage is most prominent. To further confirm the endothelium integrity, immunofluorescence of the inter-endothelial tight junctions using antibodies specific to zonula occludens (ZO) protein, claudin and VE-cadherin is in progress in our laboratory.

Finally, a number of blood parameters were measured in the SC infected mice and the study revealed some common features with severe DEN (DHF) patients such as RBC and HCT increased concentration, and transient lymphopenia.^{35,36} However no thrombocytopenia was observed in the infected mice unlike in humans where platelets drop is one of the hallmarks of DHF.³⁶ Furthermore,

neutropenia and leukopenia also described in DHF patients³⁶ were not observed in the infected mice.

In conclusion, we report here a unique mouse model of primary DENV infection using a non mouse-adapted DEN2 virus strain (namely D2Y98P-PP1) which upon SC administration to AG129 adult mice leads to systemic increased vascular permeability accompanied by a number of clinical features and parameters that resemble those described and measured in DEN patients. Our mouse model thus offers a unique opportunity to identify the molecular players involved in DEN-associated vascular leakage and elucidate its underlying mechanisms. It also represents an ideal platform to test novel prophylactic and therapeutic interventions to fight DEN.

Acknowledgements

We are very grateful to Dr David Lye from Tan Tock Seng Hospital (Singapore) for his useful insights and critical comments of the manuscript. This work was funded by the National Medical Research Council in Singapore (TCR flagship programme 'STOP Dengue', allocated to SA).

REFERENCES

- Gubler DJ. Epidemic dengue/dengue hemorrhagic fever as a public health, social and economic problem in the 21st century. *Trends Microbiol* 2002;10:100-3.
- Tolle MA. Mosquito-borne diseases. *Curr Probl Pediatr Adolesc Health Care* 2009;39:97-140.
- Halstead SB. Dengue. *Lancet* 2007;370:1644-52.
- Bhamarapravati N, Tuchinda P, Boonyapaknavik V. Pathology of Thailand haemorrhagic fever: A study of 100 autopsy cases. *Ann Trop Med Parasitol* 1967;61:500-10.
- Kurane I. Dengue hemorrhagic fever with special emphasis on immunopathogenesis. *Comp Immunol Microbiol Infect Dis* 2007;30:329-40.
- Burke DS, Nisalak A, Johnson DE, Scott RM. A prospective study of dengue infection in Bangkok. *Am J Trop Med Hyg* 1988;38:172-80.
- Leitmeyer KC, Vaughn DW, Watts DM, Salas R, Villalobos I, de Chacon, et al. Dengue virus structural differences that correlate with pathogenesis. *J Virol* 1999;73:4738-47.
- Gulati S, Maheshwari A. Atypical manifestations of dengue. *Trop Med Int Health* 2007;12:1087-95.
- Wasay M, Channa R, Jumani M, Shabbir G, Azeemuddin M, Zafar A. Encephalitis and myelitis associated with dengue viral infection. *Clin Neurol Neurosurg* 2008;110:635-40.
- Park SB, Ryu SY, Jin KB, Hwang EA, Han SY, Kim HT, et al. Acute colitis associated with dengue fever in a renal transplant recipient. *Transplant Proc* 2008;40:2431-2.
- Basu A, Chaturvedi UC. Vascular endothelium: the battlefield of dengue viruses. *FEMS Immunol Med Microbiol* 2008;53:287-99.
- Srikiatkachorn A. Plasma leakage in dengue haemorrhagic fever. *Thromb Haemost* 2009;102:1042-9.
- Kubelka CF, Azeredo EL, Gandini M, Oliveira-Pinto LM, Barbosa LS, Damasco PV, et al. Metalloproteinases are produced during dengue fever and MMP9 is associated with severity. *J Infect* 2010;61:501-5.
- Nascimento EJ, Silva AM, Cordeiro MT, Brito CA, Gil LH, Braga-Neto U, et al. Alternative complement pathway deregulation is correlated with dengue severity. *PLoS One* 2009;4:e6782.
- Srikiatkachorn A, Ajariyakhajorn C, Endy TP, Kalayanaroj S, Libraty DH, Green S, et al. Virus-induced decline in soluble vascular endothelial growth receptor 2 is associated with plasma leakage in dengue hemorrhagic fever. *J Virol* 2007;81:1592-600.
- Kanlaya R, Pattanakitsakul SN, Sinchaikul S, Chen ST, Thongboonkerd V. Alterations in actin cytoskeletal assembly and junctional protein complexes in human endothelial cells induced by dengue virus infection and mimicry of leukocyte transendothelial migration. *J Proteome Res* 2009;8:2551-62.
- Yauch LE, Shresta S. Mouse models of dengue virus infection and disease. *Antiviral Res* 2008;80:87-93.
- Sabin AB, Schlesinger RW. Production of immunity to dengue with virus modified by propagation in mice. *Science* 1945;101:640-2.
- Prestwood TR, Prigozhin DM, Sharar KL, Zellweger RM, Shresta S. A mouse-passaged dengue virus strain with reduced affinity for heparan sulfate causes severe disease in mice by establishing increased systemic viral loads. *J Virol* 2008;82:8411-21.
- Blaney JE Jr, Johnson DH, Manipon GG, Firestone CY, Hanson CT, Murphy BR, et al. Genetic basis of attenuation of dengue virus type 4 small plaque mutants with restricted replication in suckling mice and in SCID mice transplanted with human liver cells. *Virology* 2002;300:125-39.
- Bente DA, Melkus MW, Garcia JV, Rico-Hesse R. Dengue fever in humanized NOD/SCID mice. *J Virol* 2005;79:13797-9.
- Hotta H, Murakami I, Miyasaki K, Takeda Y, Shirane H, Hotta S. Inoculation of dengue virus into nude mice. *J Gen Virol* 1981;52: 71-76.
- Johnson AJ, Roehrig JT. New mouse model for dengue virus vaccine testing. *J Virol* 1999;73:783-6.
- Williams KL, Zompi S, Beatty PR, Harris E. A mouse model for studying dengue virus pathogenesis and immune response. *Immunology and pathogenesis of viral hemorrhagic fevers. Ann NY Acad Sci* 2009;1171:E12-E23.
- Schul W, Liu W, Xu HY, Flamand M, Vasudevan SG. A dengue fever viremia model in mice shows reduction in viral replication and suppression of the inflammatory response after treatment with antiviral drugs. *J Infect Dis* 2007;195:665-74.
- Tan GK, Ng JK, Trasti SL, Schul W, Yip G, Alonso S. A non mouse-adapted dengue virus strain as a new model of severe dengue infection in AG129 mice. *PLoS Negl Trop Dis* 2010;4:e672.
- Grant D, Tan GK, Qing M, Ng JK, Yip A, Zou G, et al. A single amino acid in nonstructural NS4B protein confers virulence to dengue virus in AG129 mice through enhancement of viral RNA synthesis. *J Virol* 2011;85:7775-87.
- Li Y, Song Y, Zhao L, Gaidosh G, Laties AM, Wen R. Direct labeling and visualization of blood vessels with lipophilic carbocyanine dye DiI. *Nat Protocol* 2008;3:1703-8.
- Harvey NL, Srinivasan RS, Dillard ME, Johnson NC, Witte MH, Boyd K, et al. Lymphatic vascular defects promoted by Prox1 haploinsufficiency cause adult-onset obesity. *Nat Genet* 2005;37:1072-81.
- Trung DT, Wills B. Systemic vascular leakage associated with dengue infections—the clinical perspective. *Curr Top Microbiol Immunol* 2010;338:57-66.
- Janssen HL, Bienfait HP, Jansen CL, van Duinen SG, Vriesendorp R, Schimmsheier RJ, et al. Fatal cerebral oedema associated with primary dengue infection. *J Infect* 1998;36:344-6.

32. Chaturedi UC, Dhawan R, Khanna M, Mathur A. Breakdown of the blood-brain barrier during dengue virus infection of mice. *J Gen Virol* 1991;72:859-66.
 33. Colbert JA, Gordon A, Roxelin R, Silva S, Silva J, Rocha C, et al. Ultrasound measurement of gallbladder wall thickening as a diagnostic test and prognostic indicator for severe dengue in pediatric patients. *Pediatr Infect Dis J* 2007;26:850-2.
 34. Srikiatkachorn A, Krautrachue A, Ratanaprakarn W, Wongtapradit L, Nithipanya N, Kalayanaroj S, et al. Natural history of plasma leakage in dengue hemorrhagic fever: a serial ultrasonographic study. *Pediatr Infect Dis J* 2007;26:283-90.
 35. Lee VJ, Lye DC, Sun Y, Fernandez G, Ong A, Leo YS. Predictive value of simple clinical and laboratory variables for dengue hemorrhagic fever in adults. *J Clin Virol* 2008;42:34-9.
 36. Tanner L, Schreiber M, Low JG, Ong A, Tolfvenstam T, Lai YL, et al. Decision tree algorithms predict the diagnosis and outcome of dengue fever in the early phase of illness. *PLoS Negl Trp Dis* 2008;2:e196.
-